UNIVERSITÀ DEGLI STUDI DI
NAPOLI FEDERICO II

Scuola Politecnica e delle Scienze di Base
Corso di Laurea Magistrale in Ingegneria dell'Automazione e Robotica

Nonlinear Dynamics and Control

Control of a nonlinear Tumor Growth model

Academic Year 2024/2025

Supervisor
Prof. Mario Di Bernardo

Candidate
Fiorella Maria Romano
matr. P38000265

Abstract

This paper analyzes a nonlinear tumor growth model governed by three differential equations, extended to incorporate drug absorption dynamics. The model describes tumor progression under natural growth constraints while considering the effects of externally administered medication. The pharmacokinetics of the drug are explicitly modeled to account for absorption, enhancing the biological realism of the treatment dynamics.

The study begins by examining the system's equilibria, stability properties, and potential bifurcations under varying parameters. Building on this analysis, a control strategy is developed to regulate tumor size through optimal drug administration. The proposed control approach is evaluated on both the linearized and full nonlinear models, assessing its robustness against parameter variations and external disturbances.

Finally, a comparative analysis of different control strategies is conducted, highlighting their impact on treatment efficacy and drug dosage minimization. The findings provide insights into chemotherapy optimization, emphasizing the balance between treatment efficacy and minimizing adverse effects. Future extensions include drug resistance modeling and personalized treatment strategies.

Contents

Spelling and translation errors were detected and corrected using AI tools.

Chapter 1

Model

1.1 Context

Carcinogenesis, according to the prevailing theory, is driven by mutations in the genetic material of normal cells, which disrupt the balance between cell proliferation and cell death. This results in uncontrolled cell division and tumor formation. Rapid and disorganized proliferation may lead to either benign or malignant tumors (cancer). Malignant tumors have the potential to invade other organs, spread to distant sites (metastasis), and pose a threat to the individual's life.

This process typically requires multiple mutations affecting specific classes of genes. The loss of proliferative control occurs only as a result of mutations in genes involved in regulating cell division, cell death, and DNA repair mechanisms. [1]

The selected system describes tumor growth dynamics under the influence of drug therapy. It is based on a three states nonlinear model used in oncology to characterize tumor growth patterns. The model is extended to include the dynamics of drug absorption and action, making it more biologically realistic.
This model is widely applied in the medical and pharmaceutical fields, particularly in cancer research and optimization of chemotherapy regimens.

1.2 Mathematical Model

Let $N(t)$ represent the number of normal cells at time t, $T(t)$ the number of tumor cells, and $I(t)$ the number of immune cells. The system is described by the following set of ordinary differential equations:

$$\frac{dN}{dt} = r_2 N(1 - b_2 N) - c_4 TN \tag{1.1}$$

$$\frac{dT}{dt} = r_1 T(1 - b_1 T) - c_2 IT - c_3 TN \tag{1.2}$$

$$\frac{dI}{dt} = s + \frac{\rho IT}{\alpha + T} - c_1 IT - d_1 I \tag{1.3}$$

where:

- $N(t)$: number of normal (host) cells. A decrease in N indicates the dominance of tumor cells over healthy tissue, while an increase suggests successful resistance to tumor growth.
- $T(t)$: number of tumor cells. If T increases rapidly, the tumor is growing uncontrollably, while a decrease suggests effective immune response or therapeutic intervention.
- $I(t)$: number of immune cells. A high I value means a strong immune response, whereas a low I could indicate immune suppression or exhaustion.
- r_1, r_2: growth rates of tumor and healthy cells, respectively.
- b_1, b_2: represents the maximum population size that the environment can sustain for tumor and healthy cells, respectively.
- c_1, c_2, c_3, c_4: system coefficients that characterize cell interactions. Those are positive constants, in order to assume destructive competition.
- d_1: Natural death rate of immune cells.

- ρ: activation rate of immune cells by the tumor. A large value means the immune system is highly reactive to the tumor's presence.

- α: saturation parameter for immune response. This regulates the extent to which immune cells can be stimulated by the tumor.

By selecting as state variables $x_1(t) = N(t)$, $x_2(t) = T(t)$, $x_3(t) = I(t)$, the following dynamic system is obtained:

$$\begin{cases} \dot{x}_1(t) = r_2 x_1(1 - b_2 x_1) - c_4 x_2 x_1 \\ \dot{x}_2(t) = r_1 x_2(1 - b_1 x_2) - c_2 x_3 x_2 - c_3 x_2 x_1 \\ \dot{x}_3(t) = s + \dfrac{\rho x_3 x_2}{\alpha + x_2} - c_1 x_3 x_2 - d_1 x_3 \end{cases} \tag{1.4}$$

1.2.1 Model Interpretation

The model captures the interaction between tumor and immune cells, highlighting key mechanisms:

- Normal cells grow in a logistic way. The presence of tumor cells reduces the number of normal cells through direct competition.

- Tumor cells grow logistically but are suppressed by immune activity and also by competition with normal cells.

- The immune response is stimulated by the presence of the tumor, with a non-linear activation term. The presence of a constant supply s of new immune cells enables the body, in the absence of tumor, to continuously produce new immune cells.

To ensure consistency and biological relevance, the model is normalized with respect to the total number of normal cells, set at 10^{11} cells per cm^3. The following assumptions have been adopted for the simulations in this study [2]:

- The total cell population in the tissue is normalized to 10^{11} cells per cm^3, serving as a reference scale for all other cell concentrations.
- The minimum detectable concentration of tumor cells is 10^7, representing the threshold for clinical detection.
- At the healthy steady state, the normalized immune cell concentration is 1.65 under the given parameters. Any values falling below 10% of typical levels observed in a healthy individual are considered critically low.

1.2.2 Parameters

In this project, the following table is used to carry out the simulations [2]:

Parameter	**Value**	**Unit of measurement**
b_1	1.0	$cells^{-1}$
b_2	1.0	$cells^{-1}$
c_1	1.0	$days^{-1}cells^{-1}$
c_2	0.5	$days^{-1}cells^{-1}$
c_3	1.0	$days^{-1}cells^{-1}$
c_4	1.0	$days^{-1}cells^{-1}$
d_1	0.2	$days^{-1}cells^{-1}$
r_1	1.5	$days^{-1}$
r_2	1.0	$days^{-1}$
α	0.3	$cells$
s	0.33	$cells\ days^{-1}$
ρ	0.01	$days^{-1}$

Table 1.1: Parameter Values for Tumor Growth Model

Chapter 2

Open Loop Analysis

In this chapter, the internal and structural stability of the autonomous dynamic model discussed in Chapter 1 will be analyzed.

2.1 Equilibrium point

In this section, the equilibrium points identified will be classified through the analysis of the linearized system around each equilibrium point, considering the parameters in Table 1.1. The stability of each equilibrium will be assessed by examining the eigenvalues of the Jacobian matrix that characterize the local behavior of the system near these points.

The equilibrium points of the system are given by the intersections of the nullsurfaces, obtained setting:

$$\begin{cases} f_1(x_1, x_2, x_3) = 0 \\ f_2(x_1, x_2, x_3) = 0 \\ f_3(x_1, x_2, x_3) = 0 \end{cases} \tag{2.1}$$

Hence:

$$\begin{cases} r_2 x_1(1 - b_2 x_1) - c_4 x_2 x_1 = 0 \\ r_1 x_2(1 - b_1 x_2) - c_2 x_3 x_2 - c_3 x_2 x_1 = 0 \\ s + \dfrac{\rho x_3 x_2}{\alpha + x_2} - c_1 x_3 x_2 - d_1 x_3 = 0 \end{cases} \tag{2.2}$$

Through the help of MATLAB the following intersections were found:

```
syms x1 x2 x3

eq1 = r2 * x1 * (1 - b2 * x1) - c4 * x2 * x1 == 0;
eq2 = r1 * x2 * (1 - b1 * x2) - c2 * x3 * x2 - c3 * x2 * x1 == 0;
eq3 = s + (rho * x3 * x2) / (alpha + x2) - c1 * x3 * x2 - d1 * x3 == 0;

sol = vpasolve([eq1, eq2, eq3], [x1, x2, x3]);

disp('Intersection points (x1, x2, x3):');
```

```
Intersection points (x1, x2, x3):
```

```
disp([double(sol.x1), double(sol.x2), double(sol.x3)]);
```

```
    1.2916   -0.2916    1.2916
    0.4352    0.5648    0.4352
    0.7632    0.2368    0.7632
         0         0    1.6500
    1.0000         0    1.6500
         0    0.8992    0.3023
         0   -0.2832    3.8497
         0   -0.1060    3.3180
```

Figure 2.1: Equilibria from the intersection of the three null-surfaces

Negative values of the state variables are not contemplated because they have no biological meaning, so the following equilibrium points will be considered:

Points (x_1, x_2, x_3)	**Eigenvalues**	**Type**
$(0.4352, 0.5648, 0.4352)$	$\lambda_1 = -1.3336,\ \lambda_2 = -0.0452,\ \lambda_3 = -0.6619$	Stable Node
$(0.7632, 0.2368, 0.7632)$	$\lambda_1 = 0.0515,\ \lambda_2 = -1.0747,\ \lambda_3 = -0.5276$	Saddle Point
$(0, 0.8992, 0.3023)$	$\lambda_1 = -0.8302,\ \lambda_2 = -1.6103,\ \lambda_3 = 0.1008$	Saddle Point
$(1, 0, 1.65)$	$\lambda_1 = -1.0,\ \lambda_2 = -0.2,\ \lambda_3 = -0.325$	Stable Node
$(0, 0, 1.65)$	$\lambda_1 = 1.0,\ \lambda_2 = -0.2,\ \lambda_3 = 0.675$	Saddle Point

Table 2.1: Equilibrium points and their classification

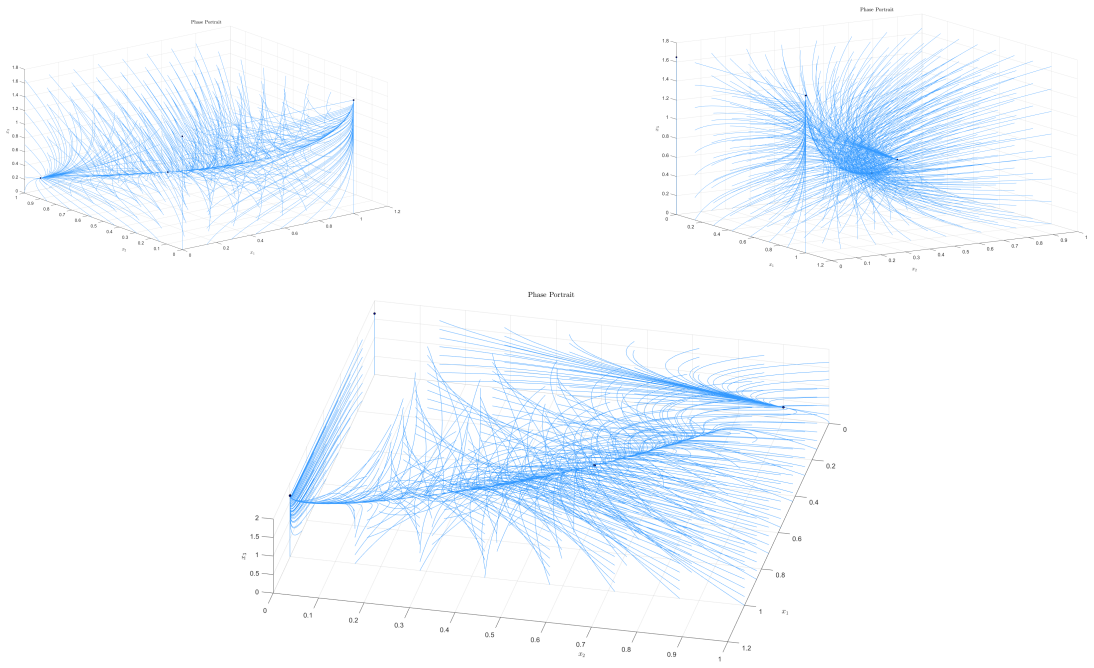

Figure 2.2: Phae Portrait of the system

The *Hartman-Grossmann theorem* states that, in the neighborhood of a hyperbolic equilibrium, the phase portrait of the linearized system is topologically equivalent to that of the original nonlinear system. Since $J_i(x^*)$ is non-singular for all i, the equilibrium points are hyperbolic, allowing the local dynamics of the nonlinear system to be analyzed through its linear approximation.

2.1.1 Biological Meaning of the Equilibrium points

Tumor Free Equilibria In the case where $x_2 = 0$, representing the absence of tumor cells, the system reaches an equilibrium point known as the tumor-free equilibrium. This point is given by $(\frac{1}{b_2}, 0, \frac{s}{d_1})$. It suggests a healthy state in which tumor cells are absent and the immune system is present at a constant and healthy level. In this scenario, the system reflects a balance where the tumor has been eradicated or never formed, and the immune system continues to function at a steady state. This also gives the healthy steady-state immune level, which is $I = \frac{s}{d_1} = 1.65$. In this scenario, the eigenvalues of J are $\lambda_1 = -1.0$, $\lambda_2 = -0.2$,

$\lambda_3 = -0.325$, so it's possible to conclude that this point is *locally stable*, since the eigenvalues are all different and have all negative real parts. A detailed Lyapunov-based stability analysis confirms local asymptotic stability for small perturbations.

Dead Equilibrium In the case where $x_1 = 0$, the system reaches an equilibrium point known as the dead equilibrium, since there are no more normal cells.
In this case, two scenarios are possible:

1. $x_2 = 0$: in this case the equilibrium point is $(0, 0, \frac{s}{d_1}) = (0, 0, 1.65)$, where both normal and tumor cells are zero.

2. $x_2 \neq 0$: the solution is given by the intersection of these two curves, so it depends on the parameters. This state represents a pathological condition where normal cells are absent (so the tissue is dead), but the tumor has not yet been eradicated and immune cells maintain their activity. This point is a saddle equilibrium since its eigenvalues have real parts but they differ in sign.

Coexisting Equilibrium The last possible scenario is the one in which both normal and tumor cells populations are non-zero. This means that small tumor mass might coexist with a large number of normal cells.
Two equilibrium point were found, which are $x_1 = (0.4352, 0.5648, 0.4352)$ and $x_2 = (0.7632, 0.2368, 0.7632)$. The first one is LS, while x_2 is a saddle point.

2.2 Stability Analysis

Lyapunov's indirect method, also known as the linearization method, makes it possible to study the local stability of the equilibrium points of a dynamical system. This approach is based on the analysis of the Jacobian matrix of the system evaluated at the equilibrium point.

However, the indirect method does not allow obtaining information on the asymptotic stability of the system. Therefore, the direct Lyapunov method is used, which is based on the construction of a Lyapunov function, a generalized energy of the system, the evolution of which over time allows the asymptotic stability of the equilibrium point to be established.

Let's consider the following equilibrium point $x^* = (1, 0, 1.65)$ and Lyapunov candidate:

$$V(\zeta) = \frac{1}{2}(\zeta - \bar{\zeta})^T P(\zeta - \bar{\zeta})$$

so that:

$$\dot{V(\zeta)} = (\zeta - \bar{\zeta})^T P\dot{\zeta}$$

where P is a diagonal, positive definite matrix and $\bar{\zeta}$ the equilibrium point. Hence:

$$V(x_1, x_2, x_3) = \frac{1}{2}[P_1(x_1 - 1)^2 + P_2x_2^2 + P_3(x_3 - 1.65)^2]$$

and

$$\dot{V}(x_1, x_2, x_3) = P_1(x_1 - 1)\dot{x_1} + P_2x_2\dot{x_2} + P_3(x_3 - 1.65)\dot{x_3}]$$

This is a good Lyapunov candidate since:

- $V : \Omega \to R^3$ is continously differentiable
- $V(\bar{x}) = 0$
- $V(x_1, x_2, x_3) > 0 \ \forall x \in R$ unless in $\bar{x}$

At the end, the result is the following:

$$\begin{aligned}\dot{V}(x_1, x_2, x_3) = &-P_1x_1(x_1 - 1)^2 - P_1x_2x_1^2 + P_1x_1x_2 + 1.5P_2x_2^2 \\ &- 1.5P_2x_2^3 - P_2x_3x_2^2 - P_2x_1x_2^2 \\ &+ P_3(x_3 - 1.65)\left(0.33 + 0.01\frac{x_3x_2}{0.3 + x_2} - x_3x_2 - 0.2x_3\right)\end{aligned} \tag{2.3}$$

This quantity is the sum of negative terms, given that the state variables are always nonnegative, with at most two positive terms (highlighted). However, by properly calibrating the P matrix, it is possible to obtain a derivative that is negative throughout the entire domain.

In particular, by setting $P_1 = 30, P_2 = 70, P_3 = 1$ it's possible to get in the neighborhood of the equilibrium point:

```
% grid details
side = 0.1;
step = 0.01;

%grid points coordinates
xi_1_vec = xi_eq(1) - side : step : xi_eq(1) + side;
xi_2_vec = xi_eq(2) - side : step : xi_eq(2) + side;
xi_3_vec = xi_eq(3) - side : step : xi_eq(3) + side;
%Vdot initialization
Vdot = zeros(length(xi_1_vec), length(xi_2_vec), length(xi_3_vec));

%Vdot copmutation
for i = 1 : length(xi_1_vec)
    for j = 1 : length(xi_2_vec)
        for h = 1 : length(xi_3_vec)
            Vdot(i, j, h) = V_dot_fun([xi_1_vec(i); xi_2_vec(j); xi_3_vec(h)], t, xi_eq, r1, r2, b1, b2, c1, c2, c3, c4, rho, alpha, s, d1);
        end
    end
end

find(Vdot > 0)

ans =

  0×1 empty double column vector
```

Figure 2.3: MATLAB results

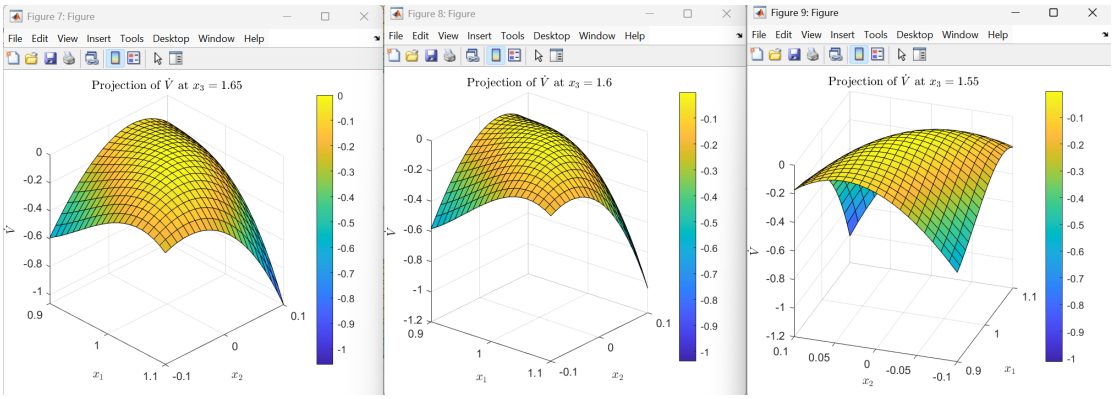

Figure 2.4: $\dot{V}$ value for different constant values of x_3

It's also possible to numerically estimate the **Region of Asymptotic Stability** (RAS) of the equilibrium point

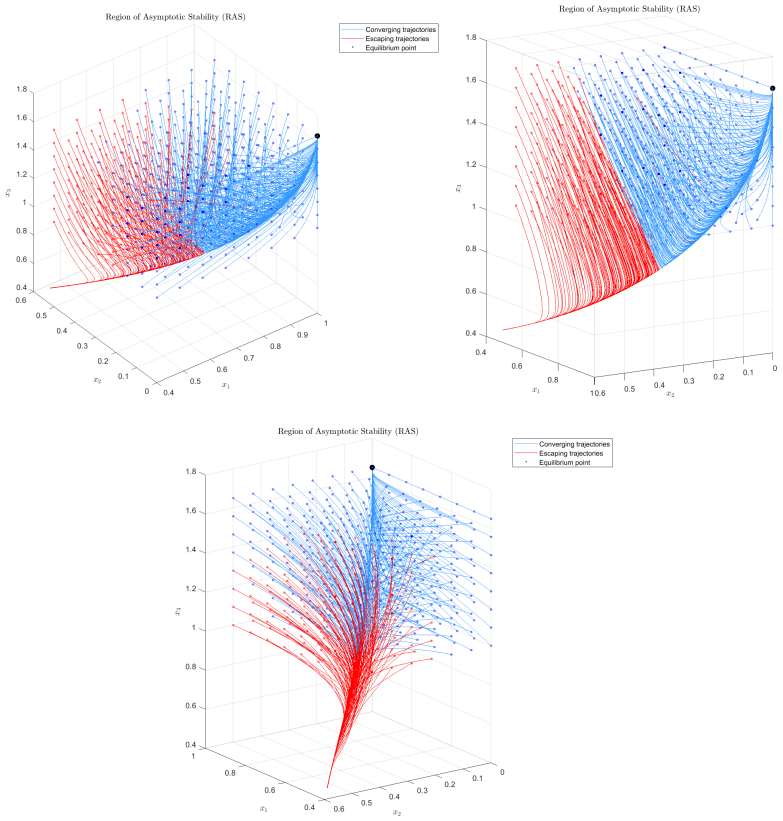

Figure 2.5: RAS estimation of $x^* = (1, 0, 1.65)$

2.3 Open-Loop simulations

In this section, simulations highlight the behavior of the autonomous dynamic system under progressively more critical initial conditions.

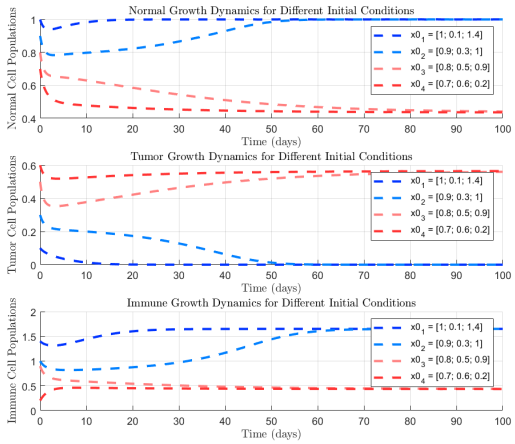

Figure 2.6: System Dynamics for Different Initial Conditions

Chapter 3

Control Synthesis

In this chapter, various techniques for controlling the system will be examined, beginning with a linear design based on the linearized model, followed by the implementation of nonlinear control. With regard to control, chemotherapy affects all cells in the body, both cancerous and non-cancerous. In particular, those cells most susceptible to division (such as cancer cells and normal cells, such as marrow cells) are affected. Consequently, the control action influences all state variables in a direct way. To account for this, a new state variable, x_4, has been introduced to represent the drug concentration at each time moment.The system is therefore defined as follows:

$$\begin{cases} \dot{x}_1(t) = r_2 x_1(1 - b_2 x_1) - c_4 x_2 x_1 - \gamma_1 x_4 \\ \dot{x}_2(t) = r_1 x_2(1 - b_1 x_2) - c_2 x_3 x_2 - c_3 x_2 x_1 - \gamma_2 x_4 \\ \dot{x}_3(t) = s + \dfrac{\rho x_3 x_2}{\alpha + x_2} - c_1 x_3 x_2 - d_1 x_3 - \gamma_3 x_4 \\ \dot{x}_4(t) = u(t) - k x_4 \end{cases} \tag{3.1}$$

where γ_i are the coefficients through which the drug acts on the cell population in question, while k is the elimination rate constant, which represents the rate at which the drug is removed from the body. It is related to the drug's half-life

($t_{1/2}$) through the equation: $k = \frac{ln2}{t_{1/2}}$. A higher value of k indicates faster drug elimination, while a lower value means the drug remains in circulation for a longer period. The control input u(t) is measured in dosage per day.

Parameter	Value	Unit of Measurement
γ_1	0.7	$dose^{-1}days^{-1}$
γ_2	1	$dose^{-1}days^{-1}$
γ_3	0.3	$dose^{-1}days^{-1}$
k	0.5	$days^{-1}$

3.1 Control Objectives

The primary objective is to effectively reduce the population of tumor cells while simultaneously safeguarding and maintaining the healthy and immune cells. For the system under consideration, a relevant objective could be to drive the system to the tumor-free equilibrium point that we have seen to be a locally asymptotically stable in a small neighborhood of the point.

The control must ensure tumor eradication by bringing the variable x_2 (tumor cells) to zero within 7 days and without overshoot. To avoid side effects and ensure sustainable therapy, the intensity of control-and thus drug delivery must be limited to a maximum value, so the following condition can be imposed: $\gamma_1 u_{\max} \ll r_2$. By substituting the given parameter values, a reasonable upper bound can be estimated as $u_{\max} \approx 1.5$. However, considering the additional effects on tumor and immune cells, a more conservative estimate is $u_{\max} \approx 0.5$. This constraint ensures that treatment is not overly aggressive, balancing efficacy and tolerability. Moreover, the following initial condition will be considered to carry out the simulations:

$$x_0 = [0.8; 0.5; 1; 0]$$

3.2 Linear Control: LQR

Linear control strategies are based on the linearization of the system around the equilibrium point:

$$\dot{x_{lin}} = A_{lin}x + B_{lin}u$$

$$y_{lin} = C_{lin}x$$

where

$$A_{lin} = J = \begin{pmatrix} \frac{\partial f_1}{\partial x_1} & \frac{\partial f_1}{\partial x_2} & \frac{\partial f_1}{\partial x_3} & \frac{\partial f_1}{\partial x_4} \\ \frac{\partial f_2}{\partial x_1} & \frac{\partial f_2}{\partial x_2} & \frac{\partial f_2}{\partial x_3} & \frac{\partial f_2}{\partial x_4} \\ \frac{\partial f_3}{\partial x_1} & \frac{\partial f_3}{\partial x_2} & \frac{\partial f_3}{\partial x_3} & \frac{\partial f_3}{\partial x_4} \\ \frac{\partial f_4}{\partial x_1} & \frac{\partial f_4}{\partial x_2} & \frac{\partial f_4}{\partial x_3} & \frac{\partial f_4}{\partial x_4} \end{pmatrix} \Bigg|_{x=x^*}, \quad B_{lin} = \begin{bmatrix} 0 \\ 0 \\ 0 \\ 1 \end{bmatrix}$$

$$C_{lin} = [0\ 1\ 0\ 0]$$

In order for a system to be completely controllable, the controllability matrix must be full rank, i.e., its rank must be equal to the order of the system n = 4. By computing the controllability matrix of the linearized system, it is possible to prove that the system is completely controllable, since it is full rank:

```
% Linearized system
J = [
    r2 * (1 - 2 * b2 * x_eq(1)) - c4 * x_eq(2) ,  -c4 * x_eq(1),   0, -gamma1 ;
    -c3 * x_eq(2),   r1 * (1 - 2 * b1 * x_eq(2)) - c2 * x_eq(3) - c3 * x_eq(1) ,  -c2 * x_eq(2), -gamma2 ;
    0,   (rho * alpha * x_eq(3)) / ((alpha + x_eq(2))^2) - c1 * x_eq(3),   (rho * x_eq(2)) / (alpha + x_eq(2)) - c1 * x_eq(2) - d1 - gamma2 , -gamma3 ;
    0, 0, 0, -k
];

B=[0; 0; 0; 1];
C=[0,1,0,0];
D=0;

% controllability
ctr = ctrb(J,B);
disp('Rank of Controllability matrix:');
```

```
Rank of Controllability matrix:
```

```
disp(rank(ctr));
```

```
     4
```

Figure 3.1: Controllability test

The linear control that will be applied in this section is the **LQR control**, which finds the optimal control law:

$$u^* = -Kx$$

where $u(t)$ minimizes the following quadratic cost function

$$J = \int_0^\infty \left(x^T Q x + u^T R u\right) dt$$

where:

- Q is a symmetric positive semi-definite weight matrix for the states,
- R is a symmetric positive definite weight matrix for the control effort.

and K is the optimal gain matrix obtained by solving the Riccati equation associated with the system.

In order to ensure a zero error at the steady state and robustness to model uncertainties, an augmented system with an integrator is considered.
The control is first designed on the linearized system and then applied on the nonlinear one (Figure 3.5). Gains found through LQR control are shown in Figure 3.2, while in Figure 3.3 is shown the stability analysis of the closed-loop system. As is possible to see, the system under the LQR control is asymptotically stable.

$$Q_i = 50;\ Q_x = \begin{bmatrix} 50 & 0 & 0 & 0 \\ 0 & 10 & 0 & 0 \\ 0 & 0 & 50 & 0 \\ 0 & 0 & 0 & 1 \end{bmatrix};\ R = 5 \tag{3.2}$$

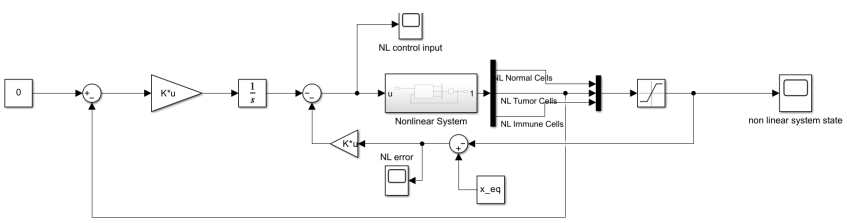

Figure 3.5: Nonlinear System with LQR control

```
[K_LQR_int, ~, Poles_LQR_int] = lqr(A_int, B_int, Q, R);

K_LQ_p = K_LQR_int(:,1:4)
```

```
K_LQ_p = 1×4
    0.0258   -5.0977    0.3238    2.7272
```

```
K_LQ_i = K_LQR_int(:,5)
```

```
K_LQ_i = 3.1623
```

Figure 3.2: LQR control Gains

```
% closed loop stability
A_cl = A_int - B_int * K_LQR_int;
eigenvalues = eig(A_cl);
disp('Eigenvalues of the closed loop system:');
```

```
Eigenvalues of the closed loop system:
```

```
disp(eigenvalues);
```

```
  -1.1884 + 1.4746i
  -1.1884 - 1.4746i
  -1.7750 + 0.0000i
  -0.5897 + 0.0000i
  -1.0108 + 0.0000i
```

```
if all(real(eigenvalues) < 0)
    disp('The system is stable under LQR control');
else
    disp('The system is not stable under LQR control');
end
```

```
The system is stable under LQR control
```

Figure 3.3: Stability analysis of the closed loop sys under LQR

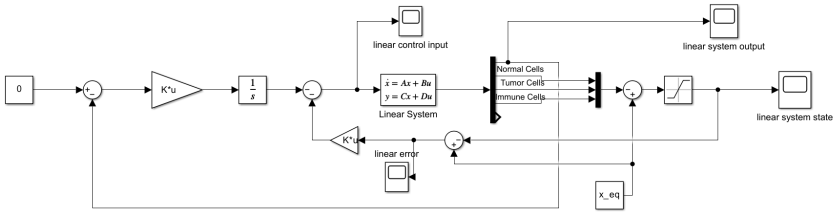

Figure 3.4: Linearized System with LQR control

3.2.1 Performance Analysis

In the following figures, the evolution of the state variables, error and control input under the LQR control law can be appreciated.

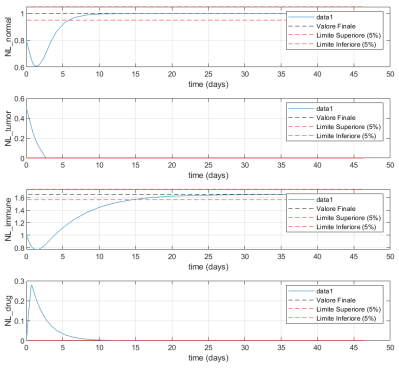

Figure 3.6: State variables evolution with LQR

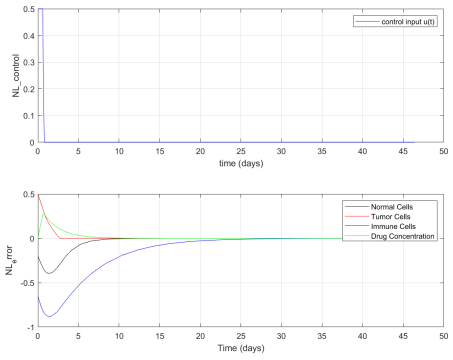

Figure 3.7: Control input and error with LQR

As can be seen from the graphs, the imposed specifications are largely met. The system takes x_2 to zero in less than 3 days, in particular in 2 days and 19 hours.

In addition, the nonlinear system resets overshoot in all simulations, bringing the state variables to steady state smoothly.

3.3 Sliding Mode Control (SMC)

Sliding Mode Control (SMC) is a robust control technique designed to control nonlinear dynamic systems. It works by forcing the system's state to "slide" along a predetermined surface, known as the sliding surface, by switching the control input in response to system states. The primary advantage of SMC is its ability to achieve robustness against system uncertainties and disturbances.

The idea behind switching control in general is to consider controllers whose structure can change according to some conditions. The result is a control input u that is not smooth.

In particular, SMC aims to design a scalar function of the state $\sigma(x)$ such that, when $\sigma(x) = 0$ the control specifications are met and the trajectories are eventually trapped in the region:

$$\Sigma := \{x \in \mathcal{R}^4 : \sigma(x) = 0\}$$

Once the state reaches the sliding surface, the system remains on it despite external disturbances, ensuring stability and desired performance, thanks to a discontinuos control action of the form:

$$u = \begin{cases} u^+(x,t) & \text{when } \sigma(x) > 0 \\ u^-(x,t) & \text{when } \sigma(x) < 0 \end{cases}$$

that makes Σ globally attractive.

Let's consider the nonlinear systems in *affine form*:

$$\dot{x} = f(x) + g(x)u$$

$$x \in \mathcal{R}^n, u \in \mathcal{R}$$

The system discussed in this project can be written in the following affine form:

$$f(x) = \begin{bmatrix} r_2 x_1(1 - b_2 x_1) - c_4 x_2 x_1 - \gamma_1 x_4 \\ r_1 x_2(1 - b_1 x_2) - c_2 x_3 x_2 - c_3 x_2 x_1 - \gamma_2 x_4 \\ s + \frac{\rho x_3 x_2}{\alpha + x_2} - c_1 x_3 x_2 - d_1 x_3 - \gamma_3 x_4 \\ -k x_4 \end{bmatrix} \quad g(x) = \begin{bmatrix} 0 \\ 0 \\ 0 \\ 1 \end{bmatrix}$$

The following scalar function was chosen:

$$\sigma(x) = p_1(x_1 - x_{1d}) + p_2 x_2 + p_3(x_3 - x_{3d}) + p_4 x_4 \tag{3.3}$$

In order to fulfill the *attractivity condition*, the following control law must be designed:

$$u = \frac{1}{\mathcal{L}_g(\sigma)}[-\mathcal{L}_f(\sigma) - Ksign(\sigma)] \tag{3.4}$$

where:

$$\mathcal{L}_g(\sigma) = \frac{\partial \sigma}{\partial x} g = \begin{pmatrix} p_1 & p_2 & p_3 & p_4 \end{pmatrix} \begin{pmatrix} 0 \\ 0 \\ 0 \\ 1 \end{pmatrix} = p_4 \neq 0 \tag{3.5}$$

in order to fulfill also the *transversality condition*, and:

$$\mathcal{L}_f(\sigma) = \frac{\partial \sigma}{\partial x} g = \begin{pmatrix} p_1 & p_2 & p_3 & p_4 \end{pmatrix} \begin{pmatrix} r_2 x_1(1 - b_2 x_1) - c_4 x_2 x_1 - \gamma_1 x_4 \\ r_1 x_2(1 - b_1 x_2) - c_2 x_3 x_2 - c_3 x_2 x_1 - \gamma_2 x_4 \\ s + \frac{\rho x_3 x_2}{\alpha + x_2} - c_1 x_3 x_2 - d_1 x_3 - \gamma_3 x_4 \\ -k x_4 \end{pmatrix} \tag{3.6}$$

This control input ensures that:

$$\dot{V}(x) = \frac{1}{2}\sigma^2(x) < 0 \ \forall \sigma(x) \neq 0$$

For the simulated system, the following parameters have been chosen:

Parameter	Value
p_1	1
p_2	1
p_3	2
p_4	15
K	20

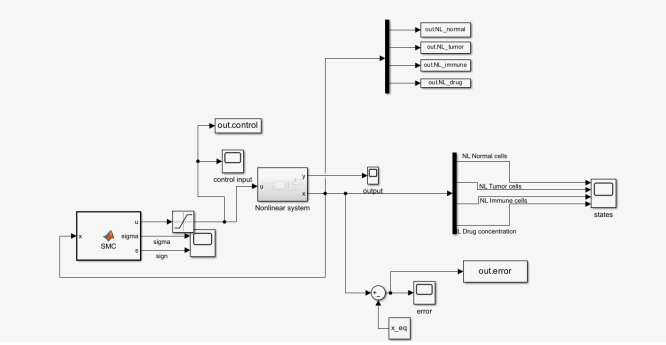

Figure 3.8: SMC Simulink scheme

3.3.1 Performance Analysis

All of the following simulations were obtained using the tanh function instead of the sign function to prevent chattering, i.e., switching between the two controls at very high, almost infinite frequencies. This allows the switching frequency to be reduced, creating a 'safety' zone (boundary layer) around the reference trajectory Σ, in which the system can operate without continuously switching between control modes.

As can be seen from the Figure 3.9 all the specifications are largely met. Nevertheless, as can be seen from Figure 3.11, control input is still affected by chattering. To mitigate this effect, the threshold ϵ has been reduced from the starting value

of $1e^{-3}$.

The result obtained is shown in Figures 3.12, 3.13. Chattering was completely abolished, but this caused the error not to converge to zero (Figure 3.14), but to take on constant steady state values, although very small.

The final results are shown in Figures 3.15, 3.16, 3.17 where is possible to see that the system takes x_2 to zero in exactly 4 days.

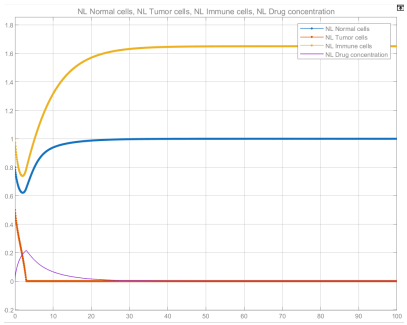

Figure 3.9: State variables with SMC and tanh function, $\epsilon = 1e - 3$

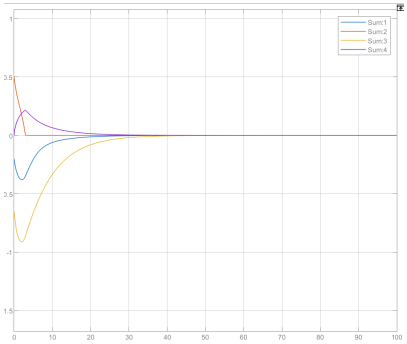

Figure 3.10: Error with SMC and tanh function, $\epsilon = 1e - 3$

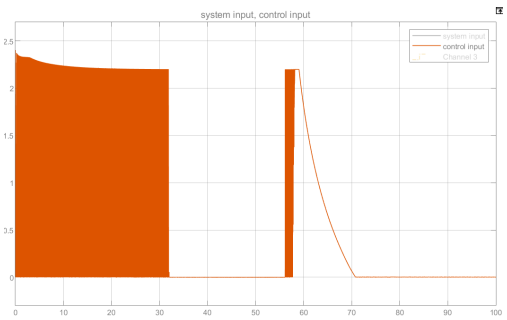

Figure 3.11: Control input with SMC and tanh function, $\epsilon = 1e - 3$

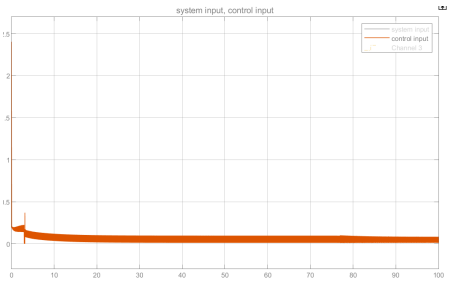

Figure 3.12: Control input with SMC and tanh function, $\epsilon = 1e-2$

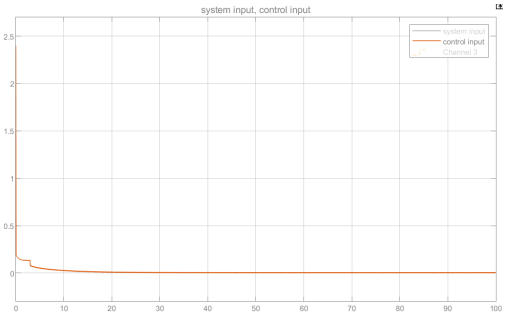

Figure 3.13: Control input with SMC and tanh function, $\epsilon = 1e-1$

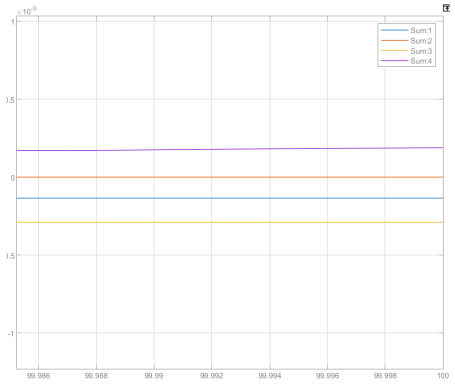

Figure 3.14: Steady state error with SMC and tanh function, $\epsilon = 1e-1$

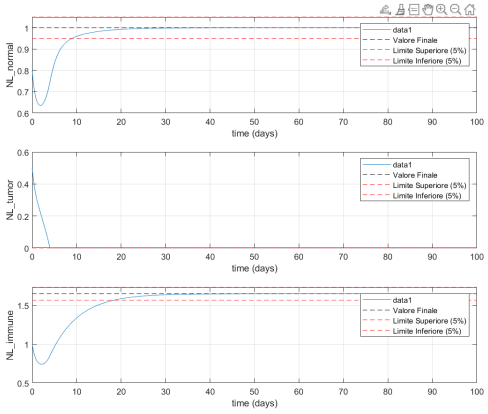

Figure 3.15: State variables with SMC and tanh function, $\epsilon = 1e-1$

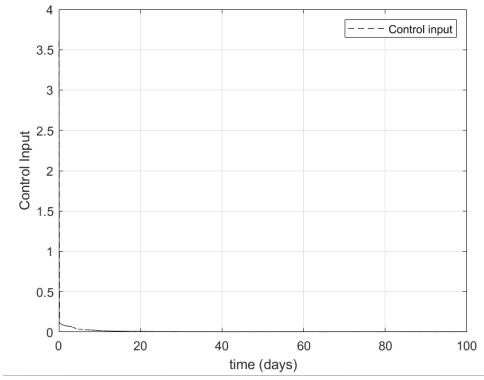

Figure 3.16: Control input with SMC and tanh function, $\epsilon = 1e-1$

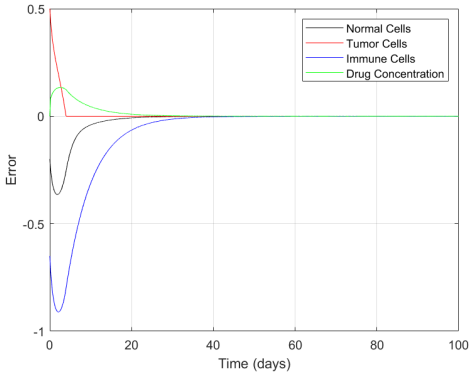

Figure 3.17: Error with SMC and tanh function, $\epsilon = 1e-1$

3.4 Nonlinear Model Predictive Control (NMPC)

Nonlinear Model Predictive Control (NMPC) is an advanced control strategy widely used in applications where system dynamics exhibit nonlinear behavior.

NMPC operates by solving an optimization problem at each time step to determine the optimal control action. The main steps in NMPC can be summarized as follows:

1. **Prediction Model**: A nonlinear dynamic model of the system is used to predict future states over a given prediction horizon N_p.

2. **Cost Function**: An objective function is defined to minimize deviations from a reference trajectory while penalizing control effort:

$$J = \sum_{k=0}^{N_p} (x_k - x_{\text{ref}})^T Q (x_k - x_{\text{ref}}) + \sum_{k=0}^{N_c} u_k^T R u_k, \tag{3.7}$$

   where Q and R are weighting matrices, and N_c is the control horizon.

3. **Constraints**: The optimization problem incorporates constraints on states and control inputs:

$$x_{\min} \leq x_k \leq x_{\max}, \quad \forall k = 0, \ldots, N_p, \tag{3.8}$$

$$u_{\min} \leq u_k \leq u_{\max}, \quad \forall k = 0, \ldots, N_c. \tag{3.9}$$

4. **Optimization and Control Application**: The optimal control sequence is computed by solving the constrained optimization problem. Only the first control input u_0 is applied to the system, and the process repeats at the next time step using updated state measurements.

The following experiments were conducted on the basis of these parameters:

$$N_p = N_c = 6$$

$$T_s = 1/24 \text{ (1 hour)}$$

$$Q = diag([10, 150, 10, 1]),\ R = 0.1$$

$$0 \leq u(t) \leq 0.5$$

$$0.3 \leq x_1(t) \leq 1,\ 0 \leq x_2(t),\ 0.3 \leq x_3(t),\ 0 \leq x_4(t)$$

The assignment of weights in the matrices ensures that the second state variable, being the one with the highest weight, does not take on high values but tends rapidly to zero. Constraints imposed on the control input limit the intensity of therapy, preventing overly aggressive approaches and ensuring biological consistency. In addition, constraints on the states prevent the values of normal and immune cells from falling below predetermined thresholds.

```
for t = 0:Ts:Tsim

    Np=min(Np,Tsim-t);
    objective = @(u) objective_fun(u, x0_new, x_eq, Q, R, p, Np, Ts);
    state_const = @(u) state_constraints(u, x0_new, p, x_max, x_min);

    options = optimoptions('fmincon','Algorithm','interior-point','MaxFunctionEvaluations',100,'MaxIterations',100);
    [u, fval, exitflag] = fmincon(objective, u_zero,[],[],[],[], u_min, u_max, state_const, options);

    u_zero = u(1);

    [t, x] = ode45(@(t, x) tumor_growth_controlled(t, x, u_zero, p), [0 Ts], x0_new);

    if x(end, 2) < 0
        x (end, 2) = 0;
    end

    x0_new = x(end, :);  % lo stato attuale sarà il prossimo stato iniziale

    X_hist = [X_hist; x0_new];
    U_hist = [U_hist; u_zero];
end
```

Figure 3.18: Matlab scripts for NMPC

3.4.1 Performance Analysis

As can be seen from the simulations in Figure 3.19, the state variables reach the desired state by meeting all specifications. in particular, the tumor cells variable goes to zero in exactly 2 days.

The control turns out to be moderate. This behavior is due to the very nature of the MPC, which, through the objective function, tends to minimize the use of the control variable.

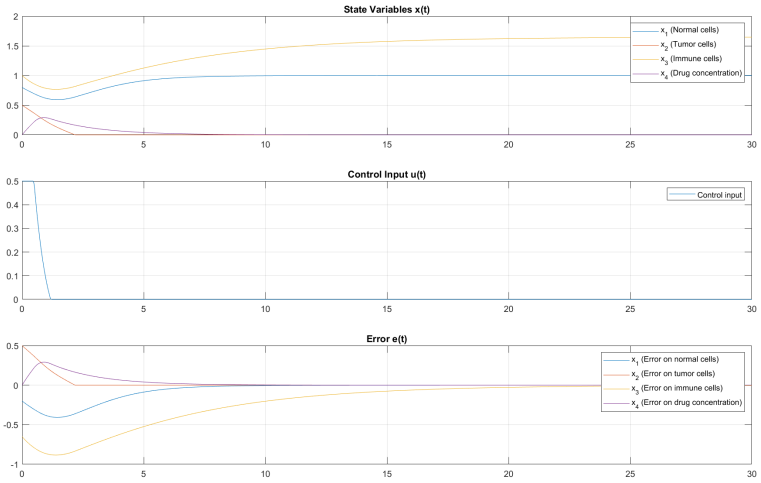

Figure 3.19: Results for NMPC

Moreover, from the plot of values that the Cost Function takes, we can see that it has a decreasing trend, that is, the algorithm finds better solutions from time to time. We can therefore conclude, in light of these considerations and from the plot of the results, that the control is stable.

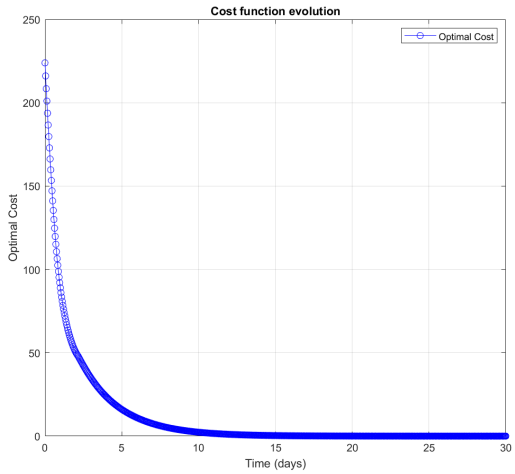

Figure 3.20: Cost Function values over time

Chapter 4

Robustness Analysis

Parameter uncertainties and disturbances pose a significant challenge on control of dynamics system because they directly affect the system's response. In this section, an error of $\pm 50\%$ on parameters c_1 and c_4 (which determine tumor aggressiveness) will be considered. As for the disturbance, on the other hand, a sinusoidal disturbance will be considered.

4.1 Linear Controller: LQR

4.1.1 Robustness to parametric uncertainties

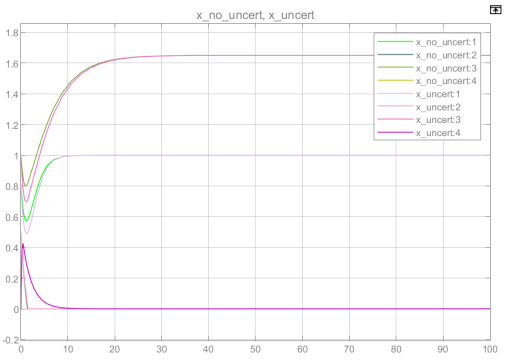

Figure 4.1: Comparison between state variables with LQR control, $+50\%$ error on c_1 and c_4 and nominal state variables

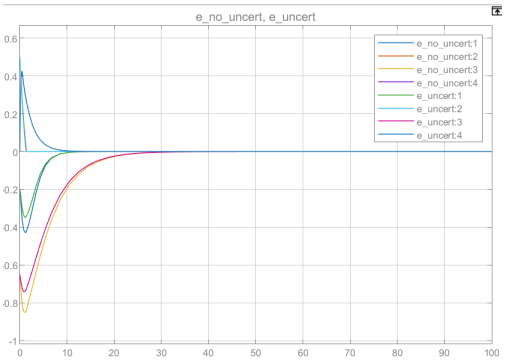

Figure 4.2: Comparison between error with LQR control, -50% error on c_1 and c_4 and nominal error

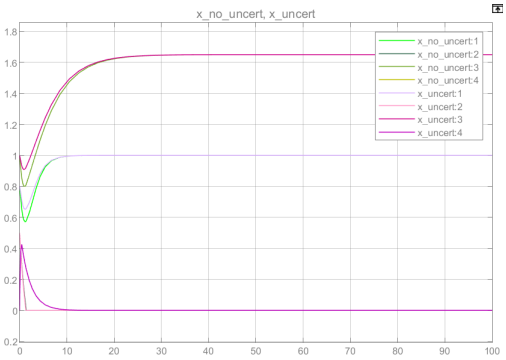

Figure 4.3: Comparison between state variables with LQR control, -50% error on c_1 and c_4 and nominal state variables

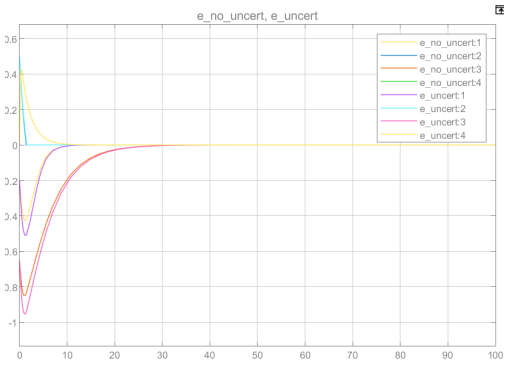

Figure 4.4: Comparison between error with LQR control, $+50\%$ error on c_1 and c_4 and nominal error

4.1.2 Robustness to disturbances

In this section, a disturb like this:

$$d_m = A_d sin(w_d t)$$

with $A_d = 1.5$ and $w_d = 0.5$ will be considered.

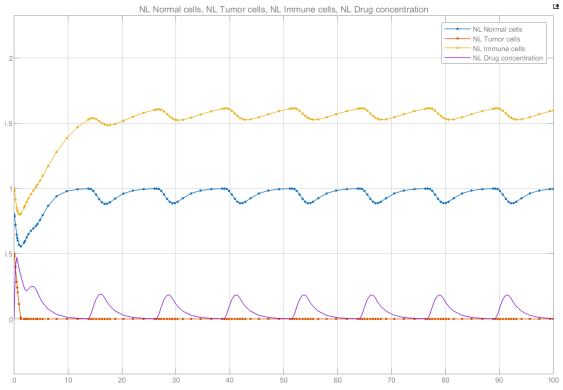

Figure 4.5: State variables with LQR control and disturb d

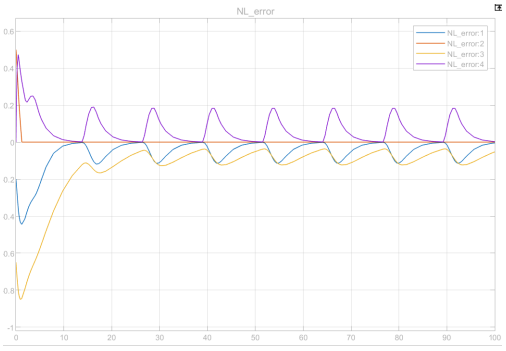

Figure 4.6: Error with LQR control and disturb d

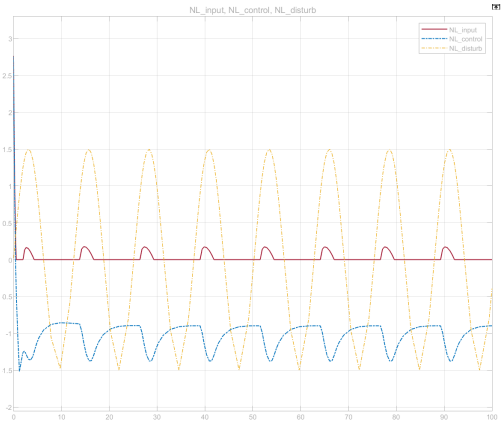

Figure 4.7: Control input and system input with LQR control and disturb d

4.2 Nonlinear Controller: SMC

4.2.1 Robustness to parametric uncertainties

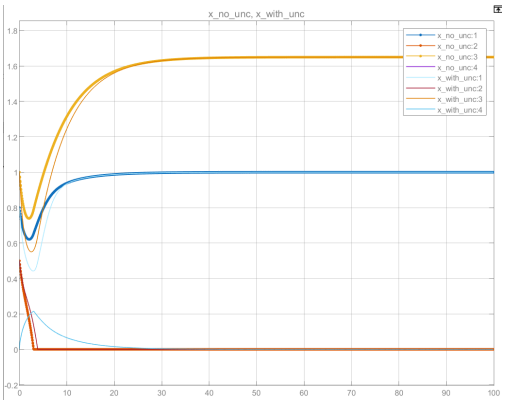

Figure 4.8: Comparison between state variables with LQR control, $+50\%$ error on c_1 and c_4 and nominal state variables

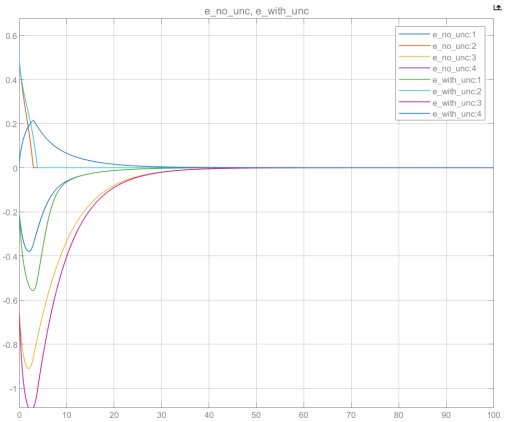

Figure 4.9: Comparison between error with LQR control, -50% error on c_1 and c_4 and nominal error

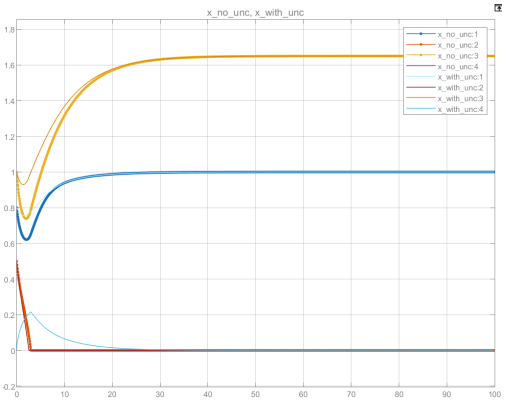

Figure 4.10: Comparison between state variables with SMC, -50% error on c_1 and c_4 and nominal state variables

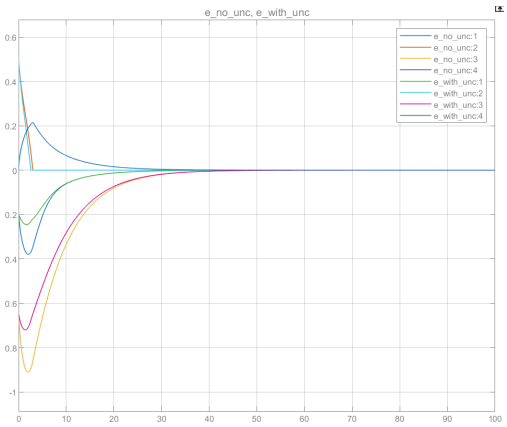

Figure 4.11: Comparison between error with SMC, $+50\%$ error on c_1 and c_4 and nominal error

4.2.2 Robustness to disturbances

Sliding Mode Control (SMC) is unaffected by matched disturbances. This means that it can perfectly compensate for those disturbances acting in the same input space as the system, i.e., in the controllable direction.

$$\dot{x} = f(x) + g(x)u + g(x)d_m$$

So, let's consider a disturb like this:

$$d_m = A_d sin(w_d t)$$

with $A_d = 1.5$ and $w_d = 0.5$. Now, the gain K of the controller must be tuned in a proper way, in order to compensate for this disturbance.

In fact, if the simulation is carried out with the same value of K used in previous chapter, the system doesn't react to the matched disturbance as expected. The results are shown in the following Figure.

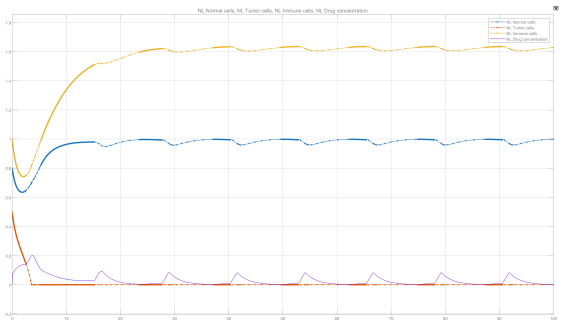

Figure 4.12: State variables with SMC, tanh function, $\epsilon = 0.1$, disturb d and $K = 20$

In the following simulation, the value $K = 70$ was suitable for rejecting the disturbance in question.

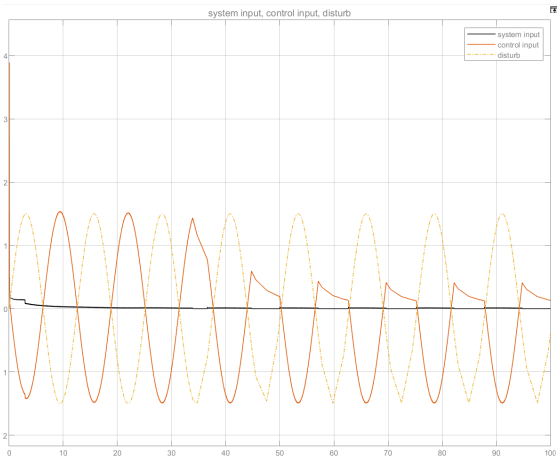

Figure 4.13: Control input, system input with SMC, tanh function, $\epsilon = 0.1$, disturb d and $K = 70$

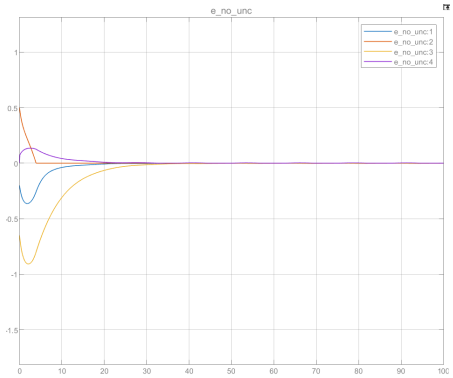

Figure 4.14: Error with SMC, tanh function, $\epsilon = 0.1$, disturb d and $K = 70$

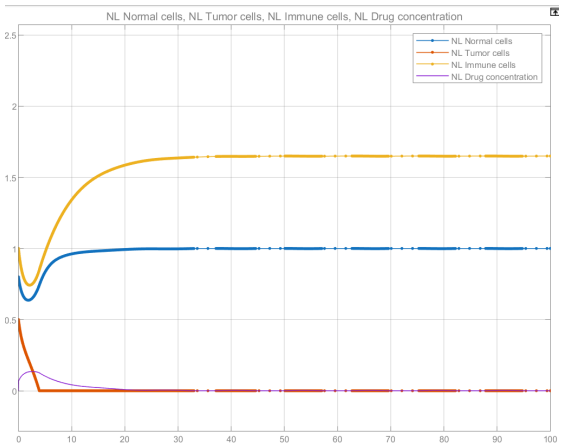

Figure 4.15: State variables with SMC, tanh function, $\epsilon = 0.1$ and disturb d

4.3 Nonlinear Controller: MPC

4.3.1 Robustness to parametric uncertainties

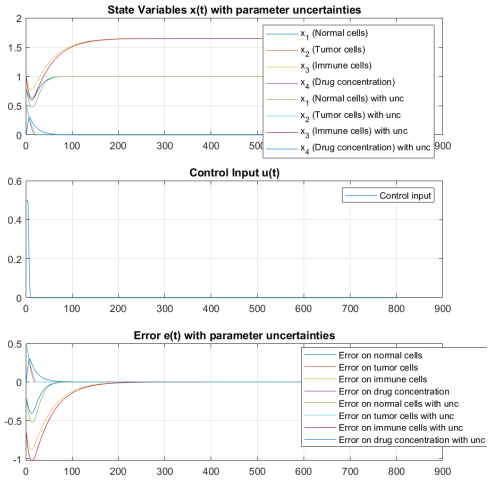

Figure 4.16: Comparison between state variables and error with MPC, +50% error on c_1 and c_4 and nominal state variables

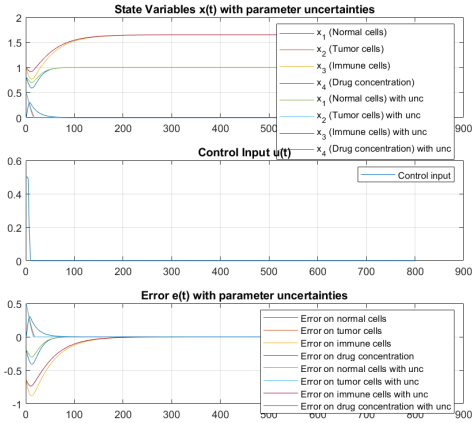

Figure 4.17: Comparison between state variables and error with MPC, -50% error on c_1 and c_4 and nominal error

4.3.2 Robustness to disturbances

Even in this case, a disturb like this one

$$d_m = A_d sin(w_d t)$$

with $A_d = 0.5$ and $w_d = 0.5$ will be considered.

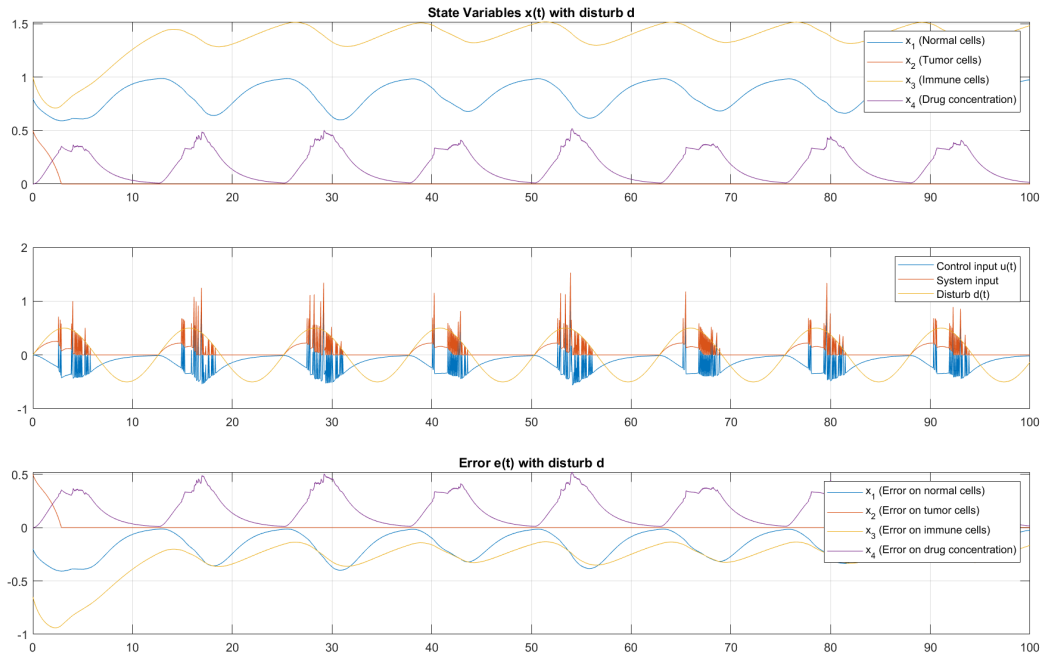

Figure 4.18: Results with MPC and disturb d

Chapter 5

Quantitative Comparison

The first controller implemented is an LQR, a linear control based on the linearized version of the original nonlinear system. Around the equilibrium point, the controller operates optimally , fully meeting the required specifications, bringing x_2 to zero in 2 days and 19 hours. In the presence of parameter uncertainties, the system responds effectively, reducing the error asymptotically to zero in a reasonable time.

When faced with a sinusoidal disturbance, the controller manages to zero out the tumor growth variable without any difficulty, while the other three state variables show fluctuations around their respective reference values. However, from the analysis of the control signal, it is observed that the system reacts by adapting to the disturbance to counter it, taking advantage of the state feedback. In addition, disturbances of lower amplitude, but with the same frequency, are attenuated without any difficulty.

-	**Ts**	**Peak in drug**
LQR	2 days 19 hours	0.27
SMC	4 days	0.28
MPC	2 days	0.13

Figure 5.1: Settling time and peak of the controllers

-	**Ts**
LQR	1 days 12 hours
SMC	4 days
MPC	2 days

Figure 5.2: Settling time of the controllers with disturbance

Among the three different controllers, the SMC is the one that converges most slowly to equilibrium, but it still meets the specifications very well bringing x_2 to zero in 4 days. Among the three controllers, it is the only one that achieves perfect disturbance rejection for all the states. In the presence of parametric errors, the behavior of the system does not seem to deviate significantly from the ideal, error-free behavior and the specifications are consistently met even in this case.

The behavior of the MPC closely resembles that of the LQR, as both algorithms aim to minimize an objective function. However, MPC has the added advantage of allowing direct incorporation of constraints on the control input and state within the optimization process. Once again, all specifications are fully met and the controller takes x_2 to zero in 2 days.

Regarding the control input, MPC and LQR exhibit very similar trends, whereas in SMC, the input gradually decreases over time. This results in a smaller peak of the state variable x_4, which has an attenuated peak of 48.15% compared to that of the control with MPC and 46,5%compared to the LQR. This means a less aggressive but more prolonged therapy. Both normal and immune cells are affected by the treatment, displaying a slower recovery trajectory.

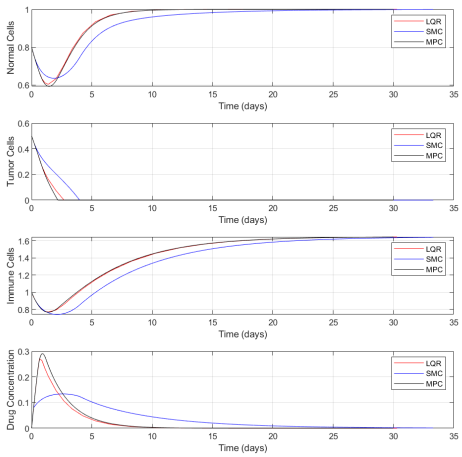

Figure 5.3: Comparison between state variables values

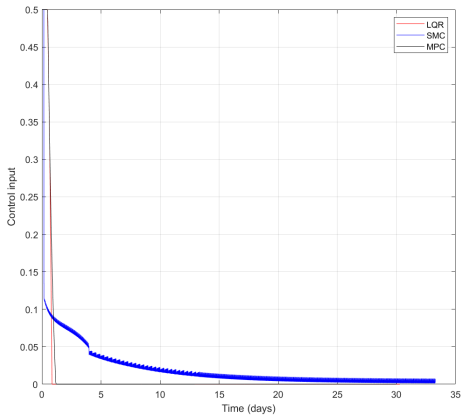

Figure 5.4: Comparison between control input values

Chapter 6

Conclusion

In this analysis, three control strategies were evaluated to regulate tumor growth using a nonlinear model. The results show that:

- LQR is an effective solution for near-equilibrium conditions, but can be sensitive to system nonlinearities in more distant regions.
- SMC offers excellent robustness to uncertainties and perturbations, providing perfect rejection of the disturbance, although it introduces chattering (partially mitigated by the tanh function).
- MPC is the most versatile, allowing constraints on state variables and control to be included, but it is computationally more onerous and requires a good predictive model.

From a therapeutic perspective, the choice of the most suitable controller depends on the clinical goals: if immediate response and aggressive therapy is desired, LQR is a good option, while if robustness to changes in parameters is a priority, SMC is preferable. If one wants to constrain levels of administered drug and minimize side effects, MPC is the most suitable choice.

Future works could involve accounting for a patient's possible relapse even after therapy or adding variables to account for the phenomenon of drug resistance.

Bibliography

[1] Wikipedia, L'enciclopedia libera.

https://it.wikipedia.org/wiki/Carcinogenesi

[2] The dynamics of an optimally controlled tumor model: A case study

https://doi.org/10.1016/S0895-7177(03)00133-X